Interferometry of a roadside DAS array in Fairbanks, AK

Eileen R. Martin, Nate Lindsey, Shan Dou, Jonathan B. Ajo-Franklin, Anna Wagner, Kevin Bjella, Tom Daley, Barry Freifeld, Michelle Robertson, and Craig Ulrich

ABSTRACT

In the summer of 2015 a shallow trenched distributed acoustic sensing (DAS) array was deployed along a road north of Fairbanks, Alaska as part of an effort to develop a low-cost system to monitor permafrost thaw under infrastructure. The dominant vibration sources were cars passing on a nearby road parallel to the array's dominant direction. Source analysis including beamforming over small frequency intervals and of the broadband recordings confirms that most noise was coming from the direction of Fairbanks or from cars. Cross-correlations of the data show unusual apparent copies of the primary Green's function, and limiting data to times with no more than one car only slightly helps these issues. Another virtual source response estimation method, cross-coherence, yields better results even with no filtering applied to the data.

INTRODUCTION

Permafrost thaw in Arctic regions can cause costly damage to infrastructure, so we are developing a low-cost system to continuously monitor the structural stability of the ground under linear infrastructure such as roads, railways, runways, and pipelines. Distributed acoustic sensing (DAS), which uses fiber optics as both a strain rate sensor and a means of transmitting that data to a central location, is becoming increasingly popular for a variety of reasons (Mateeva et al., 2013). In this context, DAS is an attractive option due to its low cost per sensor, its dense spatial sampling, its environmental resilience, and its potential for flexible geometries.

As a first step to verify that trenched DAS arrays can be used to collect anthropogenic noise, we deployed an L-shaped DAS array at Richmond, California in the winter of 2014 (Ajo-Franklin et al., 2014, 2015). Data from this array yielded reasonable cross-correlations that converged quickly (Martin et al., 2015). We developed a scalable, easily parallelizable algorithm to quickly extract dispersion images from these data (Martin, 2015), which eliminated the bottleneck of dispersion-domain surface wave inversion performed using the same method as Dou and Ajo-Franklin (2014).

In the summer of 2015 a longer array was deployed in a zone of discontinuous permafrost near Fairbanks, Alaska. The array, shown in map view in Figure 1, has a 620 meter segment running along Farmer's Loop Rd within about ten meters of the road, and loops back as a mostly parallel line. The array is about one mile north of where Johansen Expressway and Steese Highway meet, which acts as a northern boundary of Fairbanks. Steese Highway curves up and runs mostly parallel to the array about 400 meters to the east. A few geographic features of note: the area is heavily wooded and had to be cleared along parts of the array, there are some small ponds near the northern part of the array, there are several patches of asphalt near the array, there is a fence along the middle part of the array, and there are several culverts crossing the road along the array. The array was monitored by a Silixa iDAS system and ambient noise was recorded with a 1 m channel spacing and 10 m gauge length. All data analyzed in this report were collected at a 1 kHz sample rate. DAS recording had to be limited to day time only between Aug. 5 and Aug. 10.

The noise collected by the array was primarily between 5 and 25 Hz, higher than many ambient noise studies (Bensen et al., 2007; de Ridder, 2014). These higher frequencies are sensitive to more shallow features (estimates range from 1/3 wavelength to 1/2 wavelength); the features in the permafrost layer that we are concerned with are within the top 10 meters, and the typical active layer (expected seasonal thawing and freezing) is in the top meter of soil.

First, we give an overview of the data including space-time and spectral views, and beamforming results for both broadband and narrow bandpassed signals. Then, we show virtual source response estimates from cross-correlation that include some unusual features that look like copies of the expected Green's function. We hypothesize that these unusual features may be an artifact of the acquisition design: a linear array alongside a road with cars travelling parallel to the array. Then we show another virtual source response estimator, the cross-coherence, that produces results with weaker artifacts.

NOISE SOURCE ANALYSIS

The defining feature of this dataset is the presence of vehicular traffic on Farmer's Loop Rd, largely cars and trucks, as seen in Figure 2. These are the strongest noise source in all recordings because only daytime recordings are available. Using these recordings in combination with spectral stacks, we were able to pin down which channels correspond to each part of the geometry. For example, the long mostly straight line closest to the road starts with channel 535 on the south end, and extends to channel 1135 on the north end. The channels immediately before and after this line are in the opposite direction, so a single car creates a V shape in the raw data as it approaches either end of the array.

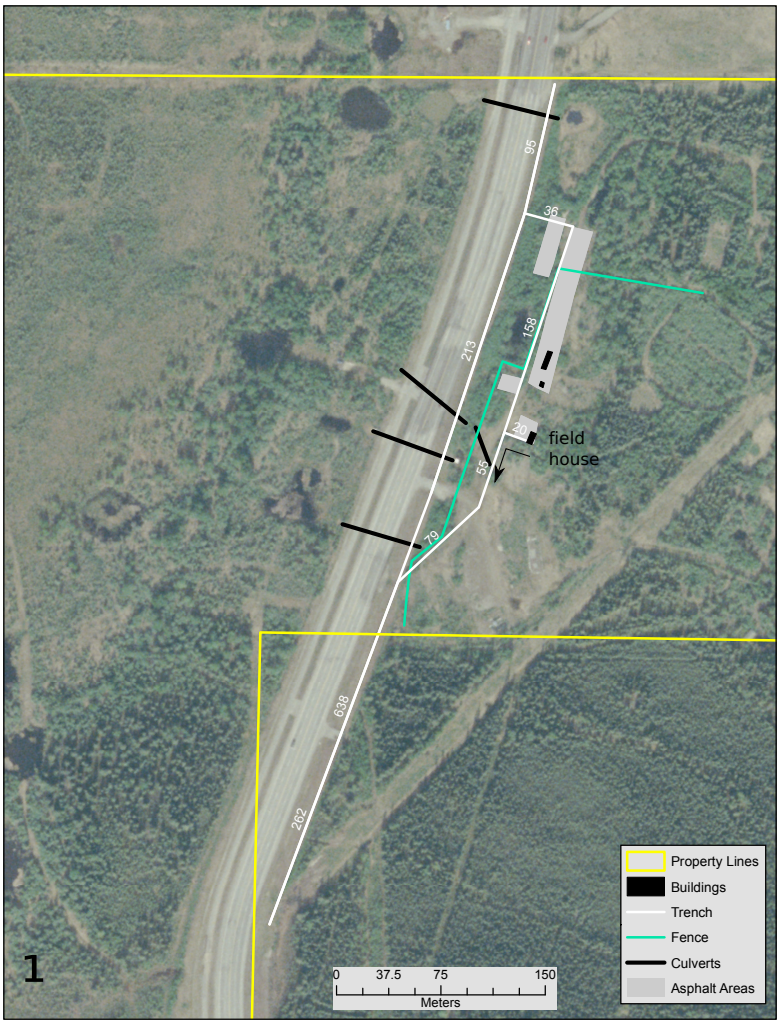

Figure 1: An overhead view of the fiber layout. Channel numbering starts at the field house and continues in the direction of the arrow. [**NR**]

The vast majority of the noise is between 3 and 50 Hz, with most noise concentrated in the 3 to 25 Hz band, as seen in Figure 3. The increase in intensity with frequency is because the interrogator unit measures strain rate traces (where that derivative multiplies the spectral amplitudes by the frequency ω). Another dominant feature (secondary to the cars) is the striping effect, which has been previously observed and is likely due to differences in the laser over different pings of the cable (stripes on all channels at once) and the conversion from optical to acoustic information (stripes on a single channel) (Ajo-Franklin et al., 2015; Martin et al., 2015).

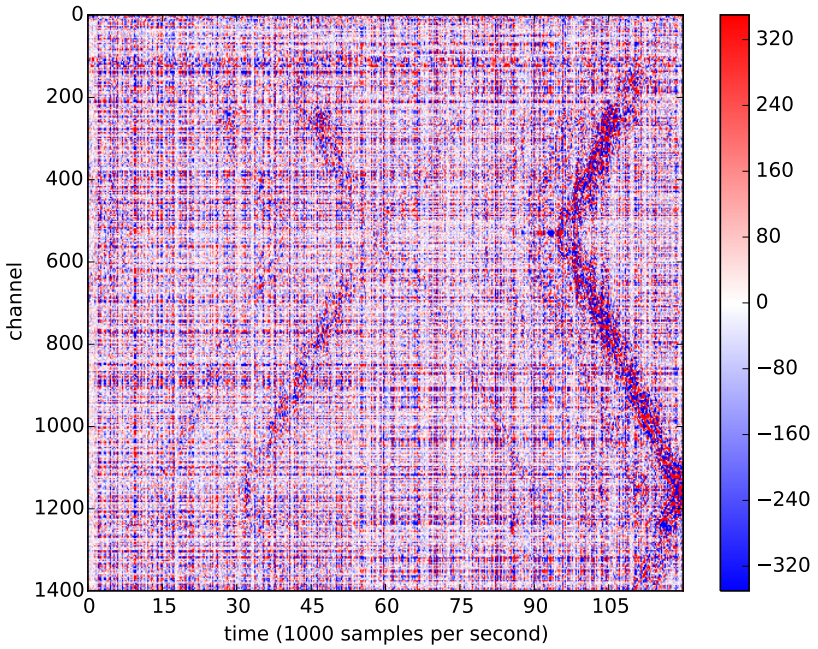

Figure 2: Several vehicles are seen passing by the array during a two minute period. First, two trucks (starting about 15 and 30 seconds into the recording) drive towards the south at roughly 22 m/s. Then several more cars including a larger truck drive towards the north. The V shapes are due to the array geometry. [**CR**]

To study where energy was coming from, we performed beamforming along the long line closest to the road. The formula used was based on Rost and Thomas (2002):

$$b(v_y) = |\sum_t \sum_r d_r(t + (y_r - y_c)v_y)|, \tag{1}$$

where v_y is any velocity of interest in the north-south direction, y_c the position of the center of the array, d_r the data recorded by receiver r at position y_r, and t time. This formula results in high b values for velocities at which there appears to be significant seismic energy propagation.

With the convention that positive velocities correspond to energy coming from the south, it is apparent that beamforming of the recorded broadband signals tend to

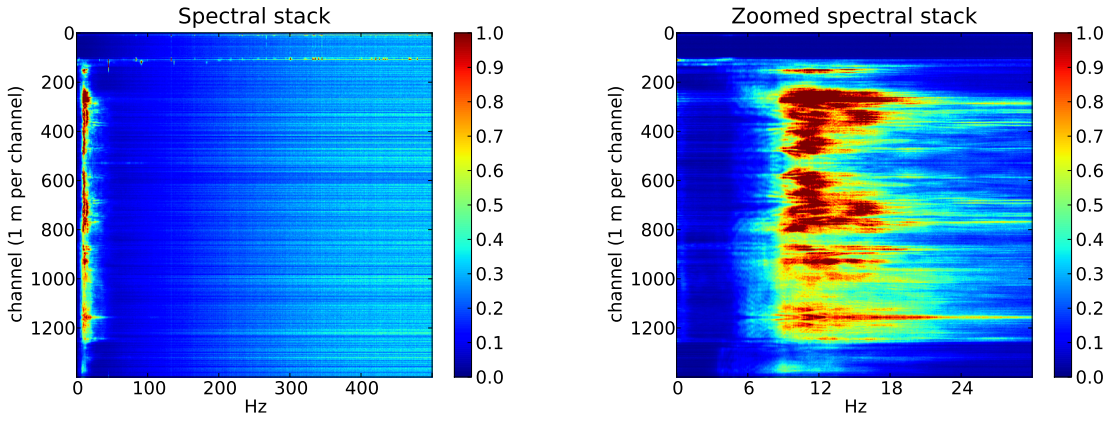

(a) (b)

Figure 3: For each channel, the spectrum stacked over a 1 hour 45 minute period during the day is shown. Nyquist frequency is 500 Hz (left) but most noise was concentrated in the 3 to 25 Hz band (right). [**CR**]

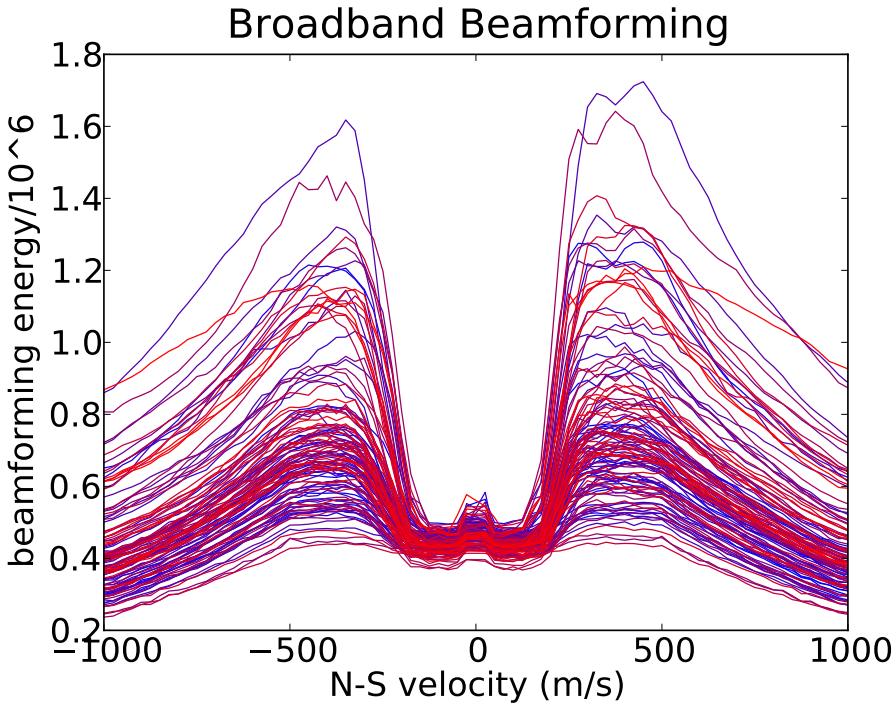

Figure 4: Beamforming on each minute of a 1 hr 45 minute daytime recording period is shown as a separate line. The trend is that more energy is coming from the south. Later minutes are shown by red lines and earlier minutes are shown in blue to show variability in energy levels over time. [**CR**]

have more energy coming from the south during most one minute recordings, as seen in Figure 4. Fairbanks is to the south of the array, so it makes sense that more noise would come from this direction. To get a better handle on how much energy of what type is coming from different directions, we performed beamforming on bandpassed signals, as in Figure 5.

It is possible, although not fully established, that the energy below 2.5 Hz is the velocity of a car moving by, and not actually energy from propagating surface waves. Between 2.5 and 15 Hz, the frequency bands that dominate the spectrum, we see a little more energy coming from the south than from the north. In the 2.5-5 Hz range, we see peaks around 600-800 m/s, but there is much less energy in this bandwidth. These beamforming results also suggest that in the 5-20 Hz range we expect to primarily have velocities around 300 to 500 m/s, which are reasonable for Rayleigh waves. Above 20 Hz, the beamformed energy decays a bit, and peaks occur in the 500-700 m/s range.

CROSS-CORRELATION ANALYSIS

A standard tool for estimating virtual source responses is the cross-correlation of filtered data recorded at all receivers with the receiver acting as a virtual source. To get good quality virtual source response estimates, it is standard to follow steps like bandpassing, whitening the spectrum of each trace, and performing temporal normalization (Bensen et al., 2007). We tried a variety of combinations of filtering procedures, but still cross-correlations of even a short time period showed unusual features that looked like copies of the expected cross-correlation at other time lags.

One procedure involved despiking the data to remove some optical noise, bandpassing (with taper) between 3 and 50 Hz, spectral whitening (up to a threshold set by the largest 80% of frequency bins), temporal normalization (by average amplitude in a moving window that is twice the longest period of interest). A result of this procedure for ten minutes of data is shown in Figure 6, and these effects tended be coherent, so they would get stronger as more time was stacked. This shows strong infinite velocity events as vertical lines, but these features can easily be removed with an FK filter, as is done in the remainder of this report.

We hypothesize that these unusual effects are due to the fact that we collect a lot of noise from car sources which are highly correlated in time. One part of this is that there are two axles on cars which causes a bit of ringing at short time lags. Another is that many cars will hit the same bumps in the road at the same distance apart, and these bumps act as little point sources within the array, which can cause extra copies of the cross-correlation. This is similar to the effect of roads within the array in Chang et al. (2014). Further modeling is being pursued to understand these issues.

To reduce the car noise while not throwing out too much data, we hand-picked an hour

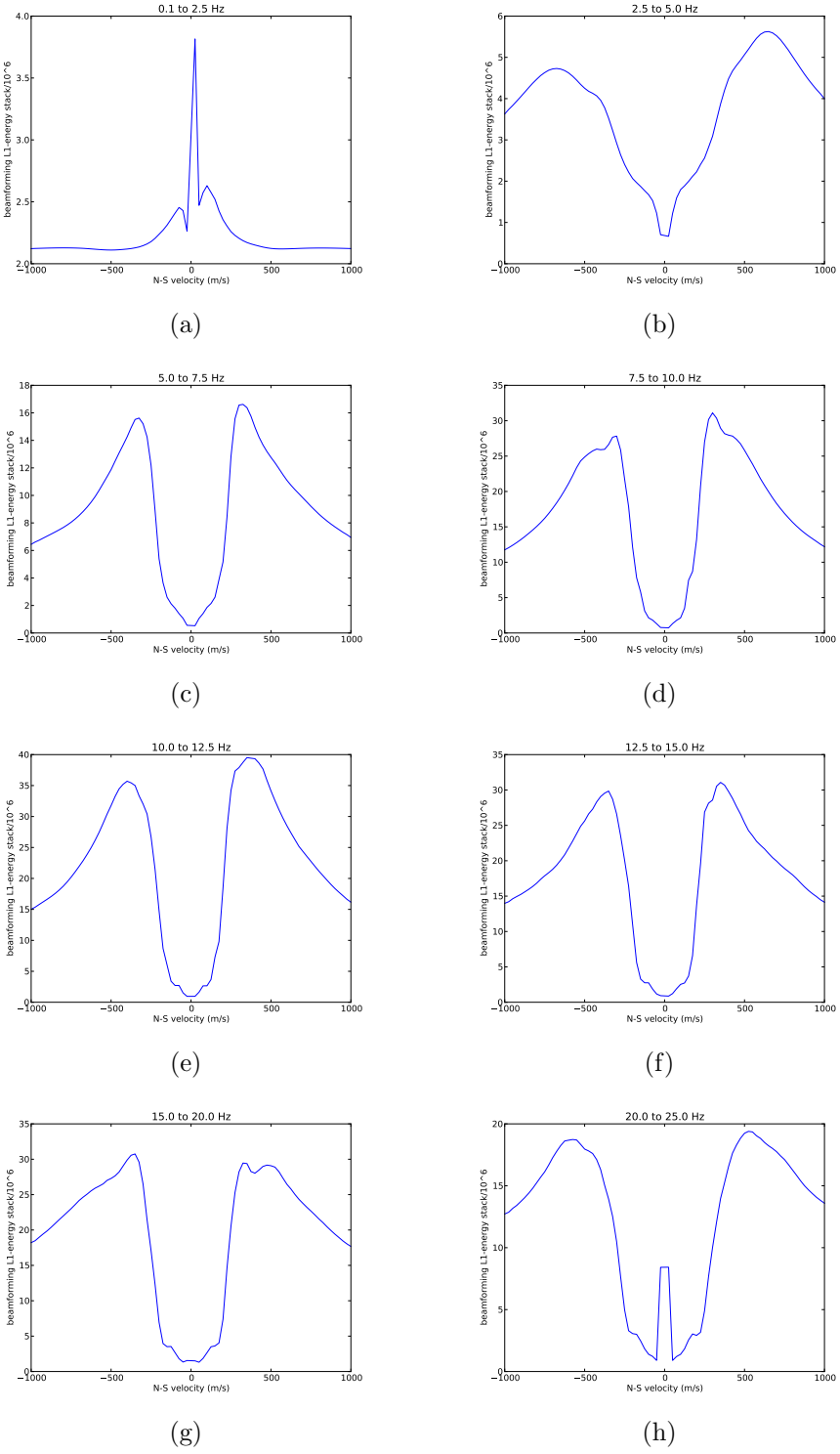

Figure 5: Beamforming results of bandpassed ambient noise were stacked over a 2 hour window for velocities between -1000 and 1000 m/s (skipping 0 velocity). First row: (left) 0.1 to 2.5 Hz, (right) 2.5 to 5.0 Hz, second row: (left) 5.0 to 7.5 Hz, (right) 7.5 to 10.0 Hz, third row: (left) 10.0 to 12.5 Hz, (right) 12.5 to 15.0 Hz, fourth row: (left) 15.0 to 20.0 Hz, (right) 20.0 to 25.0 Hz. [**CR**]

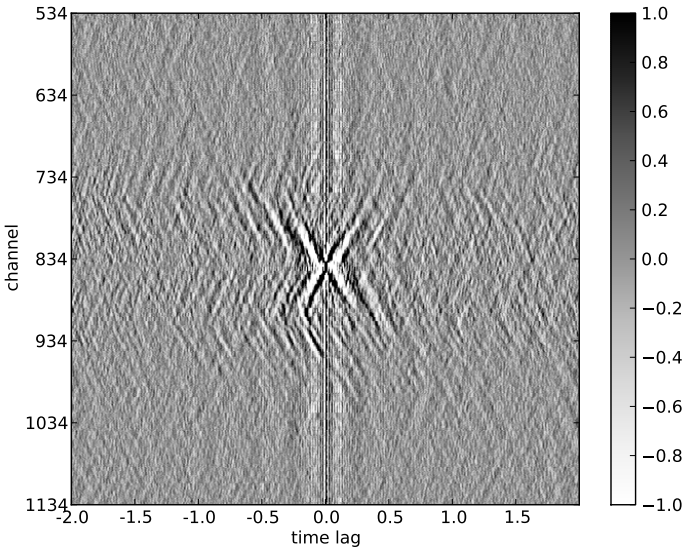

Figure 6: A cross-correlation of ten minutes of noise including any cars that were driving by shows extreme ringing and what looks like extra copies of the main virtual source response estimate. [**CR**]

of noise (out of three hours of noise) that only contained no more than 1 car passing the array at a time. We have since developed an image tracking tool to automatically detect and mute cars in the near-field of any channel. Results of cross-correlation of this hour of noise with limited cars (with the same filtering, and damping of infinite velocity events after cross-correlation) are seen in Figure 7.

CROSS-COHERENCE

Although cross-correlations are a common tool in ambient noise, and we were able to improve results by reducing the amount of car energy parallel to the array, there are other methods including cross-coherence and deconvolution that can be used to estimate virtual source response estimates. The results in Nakata et al. (2012) suggest that cross-coherence was a more effective method than cross-correlation or deconvolution for ambient noise generated in the 12-16 Hz band from nearby roads. In particular, 'ringing' artifacts in the response estimates were reduced, although their roads intersected their array perpendicularly. Cross-coherence between receivers A and B at frequency ω is defined as:

$$\frac{\hat{d}_A(\omega)\hat{d}^*_B(\omega)}{|\hat{d}_A(\omega)||\hat{d}_B(\omega)|} \tag{2}$$

where $\hat{d}_A$ is the spectrum of the data recorded at receiver A. It is quite similar to cross-correlation, but does not require us to go to such great lengths to whiten and normalize the data before comparisons. We performed cross-coherence with no

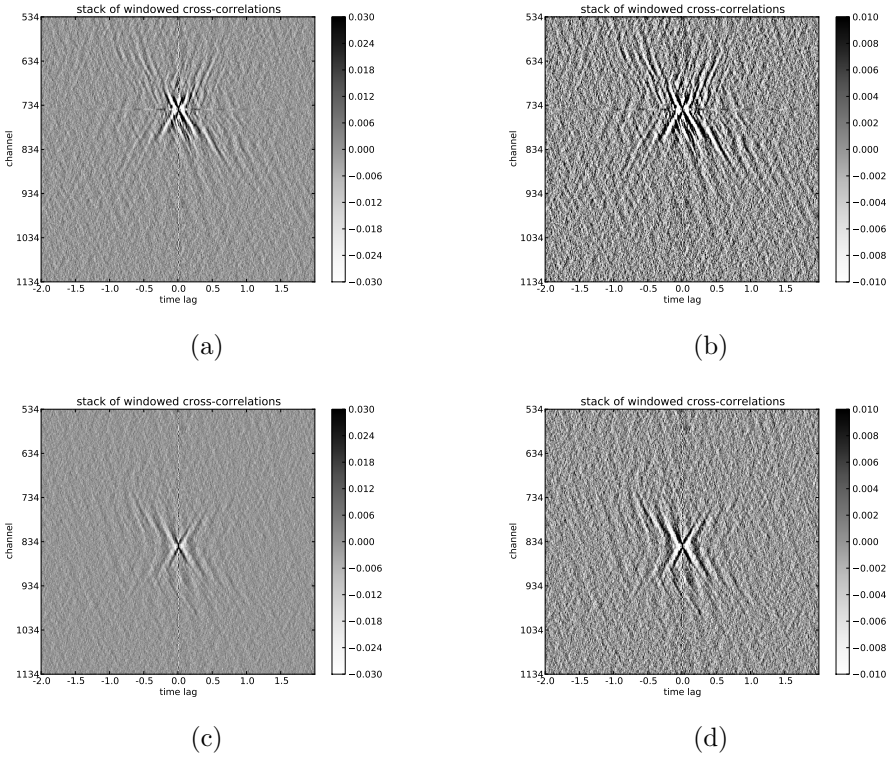

Figure 7: Cross-correlations are shown that estimate virtual source responses at channels 745 (top) and 844 (bottom). These are shown at a higher clip level (left) and a lower clip (right) to emphasize artifacts. [**CR**]

filtering on the 1 hour of hand-picked data windows with 1 or 0 cars in them, and were able to get better results than with cross-correlation that followed several filtering steps. After cross-coherence, infinite velocity events (due to optical noise occuring on all channels at once) were damped by a factor of 100, and the results are seen in Figure 8. The most noticeable improvement is that a faster event (slightly above 500 m/s) can be easily picked while it was not visible at all in the cross-correlations. This event tends to have more energy traveling from southern channels to northern channels, which is consistent with beamforming results.

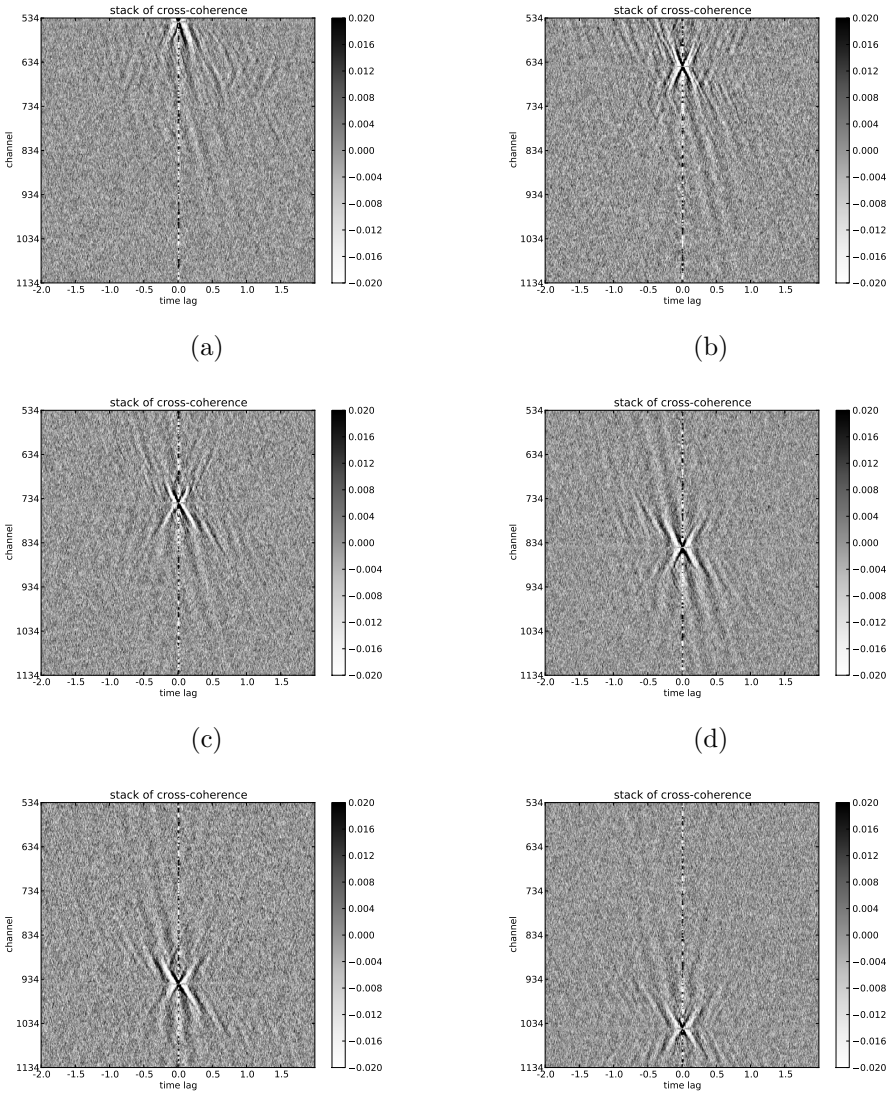

Figure 8: Cross-coherences at six virtual sources along the line closest to the road stacked over 1 hour of windows picked as having 0 or 1 cars at a time. [**CR**]

One way to improve on these dispersion images is to assume spatial stationarity within small windows, then stack cross-coherence response estimates over a small

number of nearby receivers (with the virtual sources lined up and channels shifted). This is not unreasonable considering that DAS channels already overlap. As seen in Figure 9 compared to Figure 8(d), some of the noise starts to cancel out even with just 5 neighboring virtual source response estimates stacked, although there still appear to be some artifacts, in particular the 0 time-lag crossing around channel 930-950.

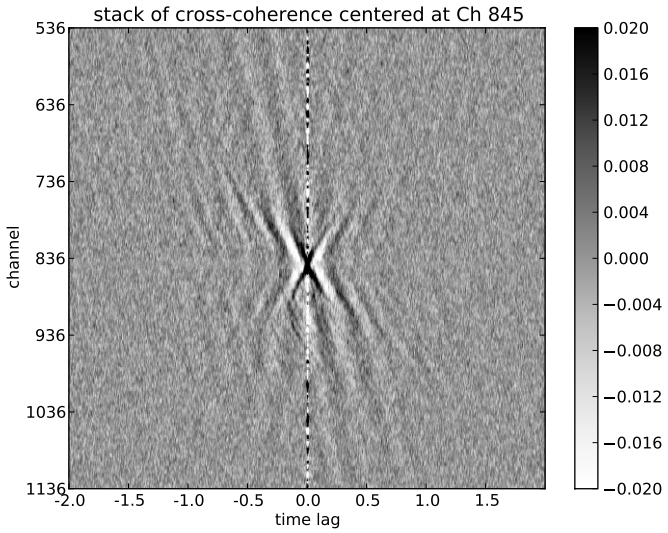

Figure 9: Virtual source response estimates for channels 843 to 847 based on 1 hr of limited car time windows were shifted to center on channel 845 then averaged. [**CR**]

Note that to get dispersion images, we can use cross-coherences, although the cross-coherences shown here were primarily for the purpose of quality control. The source spectrum information can be factored out of all cross-coherences, so it is easy to extend the $O(n)$ dispersion images algorithm from cross-correlations to cross-coherences (and even to deconvolution strategies) (Martin, 2015).

FUTURE WORK

We are currently developing synthetic models that recreate some of the artifacts observed in our virtual source response estimates. We are also refining the cross-coherence procedure to include a few filters like despiking and bandpassing that may improve the quality of the response estimates without overly modifying the data, and investigating deconvolution as an alternative. Once we have investigated whether a few more modifications can clean up the virtual source response estimates further, we look forward to calculating dispersion images so that we can perform surface wave inversion in the dispersion domain. Currently we only use information from the line closest to the road, but there are a few hundred channels away from the road at angles and parallel to the long line that we have not yet incorporated into this analysis.

CONCLUSIONS

This study revealed the difficulties of extracting virtual source response estimates from data collected by a linear DAS array running parallel to a road. In particular, apparent copies of Green's functions appeared in virtual source response estimates. Cross-coherence, even with no filtering, performed much better than cross-correlations with standard filters applied in that cross-coherence estimates had less noticeable artifacts.

ACKNOWLEDGEMENTS

The field experiments and most of the authors are supported by the US Department of Defense under SERDP grant RC-2437 "Developing Smart Infrastructure for a Changing Arctic Environment Using Distributed Fiber-Optic Sensing Methods", led by principal investigator Jonathan Ajo-Franklin at Lawrence Berkeley Lab (LBNL) and co-principal investigator Anna Wagner at the US Army Corps of Engineers Cold Regions Research & Engineering Lab. The work documented in this paper was the result of a large collaborative team involving LBNL, CRREL/ERDC, and Stanford. We would like to thank staff at the US Army Cold Regions Research and Engineering Lab for support in conducting the experiments. Eileen Martin thanks the DOE CSGF fellowship grant number DE-FG02-97ER25308 for financial support, and Jason Chang, Nori Nakata, Biondo Biondi, Bob Clapp, and Stew Levin for helpful discussions.

REFERENCES

Ajo-Franklin, J., T. Daley, B. Freifeld, D. Tang, R. Zhang, A. Wagner, S. Dou, N. Lindsey, K. Bjella, and R. Pevzner, 2014, Development of a surface-wave imaging system for geotechnical applications based on distributed acoustic sensing (DAS) and ambient noise interferometry. Presented at AGU Fall Meeting.

Ajo-Franklin, J., N. Lindsey, S. Dou, T. Daley, B. Freifeld, E. Martin, M. Robertson, C. Ulrich, and A. Wagner, 2015, A field test of distributed acoustic sensing for ambient noise recording: Expanded Abstracts of the 85th Ann. Internat. Mtg.

Bensen, G., M. Ritzwoller, M. Barmin, A. Levshin, F. Lin, M. Moschetti, N. Shapiro, and Y. Yang, 2007, Processing seismic ambient noise data to obtain reliable broadband surface wave dispersion measurements: Geophysics Journal International, **169**, 1239–1269.

Chang, J., N. Nakata, R. Clapp, B. Biondi, and S. de Ridder, 2014, High frequency surface and body waves from ambient noise cross-correlations at Long Beach, CA: Expanded Abstracts of the 84th Ann. Internat. Mtg.

de Ridder, S., 2014, Passive seismic surface-wave interferometry for reservoir-scale imaging: PhD thesis, Stanford University.

Dou, S. and J. Ajo-Franklin, 2014, Full-wavefield inversion of surface waves for mapping embedded low-velocity zones in permafrost: Geophysics, **79**, EN107–EN124.

Martin, E., 2015, Fast dispersion curves from ambient noise: SEP-Report, **158**, 255–262.

Martin, E., J. Ajo-Franklin, S. Dou, N. Lindsey, T. Daley, B. Freifeld, M. Robertson, A. Wagner, and C. Ulrich, 2015, Interferometry of ambient noise from a trenched distributed acoustic sensing array: Expanded Abstracts of the 85th Ann. Internat. Mtg.

Mateeva, A., J. Lopez, J. Mestayer, P. Wills, B. Cox, D. Kiyashchenko, Z. Yang, W. Berlang, R. Detomo, and S. Grandi, 2013, Distributed acoustic sensing for reservoir monitoring with VSP: The Leading Edge, **32**, 1278–1283.

Nakata, N., R. Snieder, T. Tsuji, K. Larner, and T. Matsuoka, 2012, Shear wave imaging from traffic noise using seismic interferometry by cross-coherence: Geophysics, **76**, SA97–SA106.

Rost, S. and C. Thomas, 2002, Array seismology: methods and applications: Reviews of Geophysics, **40**, 2–1–2–27.